34th Annual International Conference of the IEEE EMBS
San Diego, California USA, 28 August - 1 September, 2012

Analyzing gait pathologies using a depth camera

Hoang Anh Nguyen, Edouard Auvinet, Max Mignotte, Jacques A. de Guise and Jean Meunier

***Abstract*— In this paper, we present a new approach to construct a 3D human skeleton model, which is then used to quantify gait pathologies, using a depth camera. First, thanks to the depth map, we obtain a human depth silhouette in 3D, from which our method is based to estimate each body part position. Second, the angle between the upper and lower legs of the 3D skeleton model is calculated. Finally, we show that using only this angle information is enough to quantify motion asymmetry. This result has been verified through an experimental study with 3 different subjects. Due to its advantages (simple, markerless and low-cost), this method is a promising solution for gait clinics in the future.**

I. Introduction

Nowadays, in order to diagnose abnormal gait patterns in medical clinics, gait analysis systems play a crucial role [3,4,5,8,9,10]. Among state-of-the-art systems, motion capture (MOCAP) is without a doubt the most popular one due to its very high precision. Each patient is asked to wear several infrared (IR) reflective markers so that multiple IR cameras can observe the signal. Such systems cost a lot and require complex knowledge from the operator to make it function properly.

In this paper, a new gait analysis system composed of a treadmill associated with a cheap depth sensor (Kinect [11]), much simpler to implement, is proposed based on our previous works [7,16]. This system automatically constructs the 3D skeleton model of the patient walking on the treadmill. Gait asymmetry problems are detected by observing the angle variation between the upper and lower legs for each leg through time. Compared to the standard MOCAP systems, our system brings several advantages while ensuring sufficient precision for diagnosis. It does not need markers anymore, its cost is very affordable and the operator needs less time to learn it.

Before introducing our methodology in details, we make a brief summary of three basic techniques on which our whole methodology leans. These are k-means, RANSAC and polynomial least squares fitting which are introduced sequentially in the next sections.

II. K-means

In order to solve a clustering problem, k-means [14] is considered one of the simplest and most popular unsupervised learning algorithm. Given a dataset and a fixed number of clusters k, we define k centroids that represent k clusters. At each iteration, we reassign each point in the dataset to its nearest cluster, then recalculate the new position for those k centroids. The process continues until there is no change of position of the k centroids. Mathematically, given a dataset with n points $(x_1, x_2, ..., x_n)$, this algorithm aims to minimize the objective function as follows

$$f = \sum_{j=1}^{k} \sum_{i=1}^{n} \|x_i^j - c_j\|^2$$

where $\|x_i^j - c_j\|^2$ is the Euclidean distance between a data point x_i^j and the cluster centre c_j.

In our algorithm, we chose this technique for solving our clustering problem due to its easiness-to-implement and simplicity.

III. RANSAC

RANSAC is a resampling technique that generates candidate solutions by using the minimum number of observations (data points) required to estimate the underlying model parameters and iteratively enlarges this set with consistent data points.

Given a fitting problem with a vector of parameters $\vec{x}$, M data points in total, and N, the minimum number of points required, the basic algorithm is summarized as follows:

1) Select randomly N data points to determine $\vec{x}$
2) Solve for the parameters $\vec{x}$ of the model
3) Determine how many points from the set of all points fit with a user predefined tolerance.
4) If the fraction of the number of inliers over the total number points M in the set is big enough, accept the result and exit with success.
5) Repeat steps 1 through 4, L times
6) Otherwise, exit with failure

RANSAC is capable of doing robust estimation of the model parameters. Regardless of how many outliers exist in the dataset, it can find a good estimation with a high degree of accuracy. But to get such accuracy, there is a trade-off, it requires more time to compute the result. Another disadvantage of RANSAC is that the stopping condition in step 4 is really problem-specific, a general threshold that works for all cases doesn't exist.

Readers interested in RANSAC technique in detail are referred to [12].

IV. Least squares fitting

This section gives a brief explanation about polynomial least squares fitting [13]. Given a set of 2D points (x_i, y_i),

Hoang Anh Nguyen, Edouard Auvinet, Max Mignotte and Jean Meunier are with the Department of Computer Science and Operations Research, University of Montreal, Montreal (QC) Canada, H3C 3J7. Jacques A. de Guise is with the Ecole de Technologie Superieure, Montreal (QC) Canada, H3C 1K3.

978-1-4577-1787-1/12/$26.00 ©2012 IEEE

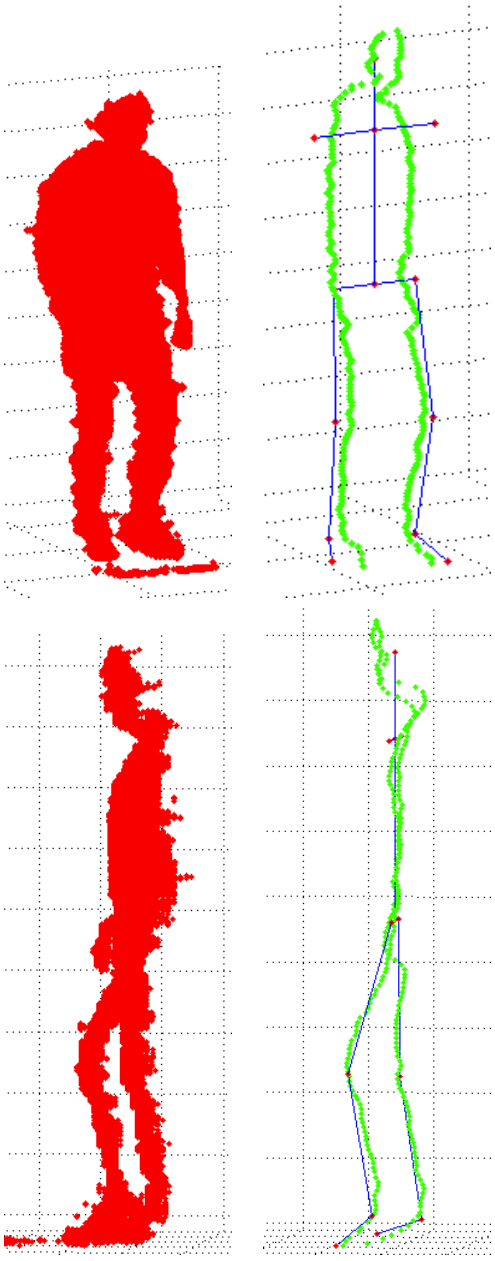

Fig. 1. Result of the 3D human skeleton construction from two different points of view. The estimation result is quite efficient in detecting the direction of both upper leg and lower leg, this allows an accurate angle calculation.

we wish to find the coefficients of a polynomial $p(x)$ of degree k that fits the data in a least squares sense.

$$y = a_k x^k + a_{k-1} x^{k-1} + ... + a_1 x + a_0$$

We form the Vandermonde matrix, V, whose elements are powers of x

$$V = \begin{pmatrix} 1 & x_1 & x_1^2 & \cdots & x_1^{k-1} \\ 1 & x_2 & x_2^2 & \cdots & x_2^{k-1} \\ \vdots & \vdots & \vdots & \ddots & \vdots \\ 1 & x_k & x_k^2 & \cdots & x_k^{k-1} \end{pmatrix}$$

In matrix notation, the equation for a polynomial fit is given by:

$$\vec{y} = V\vec{a}$$

This matrix equation can be solved numerically, or can be inverted directly if it is well formed, to yield the solution vector:

$$\vec{a} = (V^T V)^{-1} V^T \vec{y}$$

V. Gait analysis methodology

A. Experimental setup

The gait analysis system is composed of a treadmill associated with a cheap depth sensor (Kinect [11]). This system automatically constructs the 3D skeleton model of the patient walking on the treadmill. The depth images were recorded at 30 frames per second with a resolution of 640 per 480 pixels. The Kinect was placed in front of the subject and rotated 90 degrees around the optical axis in order to make the width of the image corresponds to the height of the subject. The optical axis of the camera was parallel to the translation vector of the treadmill belt.

B. Modelling the leg in 3D

This section aims to describe how to construct a 3D skeleton model starting from a depth image as the input. The structure of this image is a 2-dimensional array where each point represents its depth value. So for each image point, we get this information: horizontal coordinate u, vertical coordinate v, depth value Z. First of all, with the known camera parameters: focal distance and image centre coordinates, (f, u_0, v_0), we computed the corresponding 3D coordinate (X, Y, Z) by using the perspective transformation.

$$X = \frac{(u - u_0)Z}{f}$$

$$Y = \frac{(v - v_0)Z}{f}$$

$$Z = Z$$

The result of this transformation was a set of 3D points that describes the 3D scene for every visible point in the scene. We then manually isolated the volume of the human body, knowing its 3D position within a 3D bounding box. We used a simple 3D skeleton model consisting of 13 nodes (see figure 1). We assumed that the length of each segment was known for each individual or from anthropometric data [15]. In this study, we focused on the lower part of a human body which contains the pelvis, knees and feet. The head and arm were not required. The details of the algorithm can be found in Algorithm 1.

In order to detect the horizontal slice representing the shoulders, we observed that, when scanning each slice starting from the head downward, the width of each slice began increasing significantly from the neck to the shoulders, but remained almost the same after that. This is the key idea of

step 1 of the algorithm. In step 6, when the known length of the upper leg is reached at the knee joint then we continue with the lower leg.

Algorithm 1 Pseudo-code for constructing the 3D skeleton model

1: Detect the shoulders by observing the variation of each slice's width. When this variation becomes below a threshold, return the centre of this slice p_s
2: Initialize the 3D skeleton model based on the real shoulder width w
3: Calculate the principal components c_x, c_y, c_z for the upper half of the body. c_z gives the orientation of the torso.
4: Place node number 2 of the 3D model at p_s and node number 3 along the c_z axis at a distance corresponding to the known length of this segment. As a result, we get the position for both left $P_{leftpelvis}$ and right pelvis nodes $P_{rightpelvis}$
5: Apply the k-means with $k = 2$ for each slice below the pelvis. This helps us reduce the search space, but still well preserves the centre lines of the leg
6: Finally, for each group centroid, estimate a unit direction vector $\vec{v}$ using RANSAC + 3D line fitting.

$$P_{leftknee} = P_{leftpelvis} + \vec{v}_{leftknee} * length_{upper}$$

$$P_{rightknee} = P_{rightpelvis} + \vec{v}_{rightknee} * length_{upper}$$

$$P_{leftfoot} = P_{leftknee} + \vec{v}_{leftfoot} * length_{lower}$$

$$P_{rightfoot} = P_{rightknee} + \vec{v}_{rightfoot} * length_{lower}$$

C. Calculating the angle between the upper and lower legs

After constructing the 3D skeleton model, it was very easy to compute the angle between the upper and lower legs. This was done quickly by calculating their 2 direction vectors $\vec{v}_1$ and $\vec{v}_2$, then the angle is given by

$$\alpha = \arctan \frac{|\vec{v}_1 \times \vec{v}_2|}{\vec{v}_1 \cdot \vec{v}_2}$$

D. Cycle comparison

Until now, we have calculated the angle between upper and lower legs at every frame. As shown in figure 2A, the variations of these angles through time are sinusoid-like, and correspond to walk cycles. This reflects the fact that, during a gait period, the angle reaches its maximum when the foot is on the ground, and reduces to its minimum when the foot is up. By analyzing this variation, we observed that there was only one minimum point in a cycle. This is the key idea for the following procedure, to make the comparison process more reliable.

1) Isolating each cycle: Through time, the angle variation of each cycle was not exactly the same due to several reasons, e.g. poor angle measurement at a particular time, or sudden change in the walk pattern etc... This is the reason why we needed to isolate each cycle, and to combine them all together, to calculate the final 'mean' cycle that gives a general view of how the variation looks like for an individual. Furthermore, we also decided to eliminate all noisy points in time when the angle exceeded an upper bound found experimentally to be 160 degrees. In the next section, we describe how to align these cycles to compute the mean cycle.

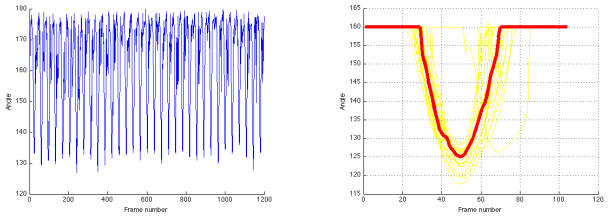

A B

Fig. 2. (A) Variation of angle between the upper and lower legs through time. A cycle starts from the lowest angle. (B) All cycles are isolated and aligned according to minimum points. The red curve represents the 'mean' cycle. Noisy high values above 160 ° degree are not displayed.

2) Aligning all cycles: Recalling that there was only one minimum per cycle, we aligned all cycles according to this minimum point. Because the data are discrete when captured at specific points in time, we applied polynomial least squares to estimate the curve that best fitted the discrete variations of the angle, and with this new continuous information, found the minimum. After some experiments on real data, we found that choosing $k = 5$ was the most suitable value for the degree of the polynomial.

The task was then much simpler, i.e. aligning all cycles according to the minimum. The results were very promising in the sense that we now clearly see in figure 2 how the angle reduces to its minimum and increases afterward for all cycles. The final task was to compute the 'mean' cycle, that is a cycle formed by taking a mean value at each point in time (Fig. 2B).

VI. Results and Discussion

In order to test our algorithm, we have captured some videos of individuals walking with the system described in section I. Each subject participating in the video acquisition was asked to wear a heel cup (height of 2.5 cm) to simulate an asymmetric walk. There was a total of 3 different videos captured separately for each person. The first video, corresponded to the normal walk without the heel cup, the second video, the heel cup was under the left foot and the last video, the heel cup was under the right foot. We have tested our methodology on 3 different subjects to demonstrate the robustness of our algorithm. Comparison results can be found in figure 3. There is a clearly visible difference between a normal walk and the heel cup walk. This allows to distinguish a normal walk from a limping walk, leading to a successful unbalanced gait diagnosis.

VII. Conclusions

In this paper, we have proposed a new technique for gait analysis based on depth information acquired from a

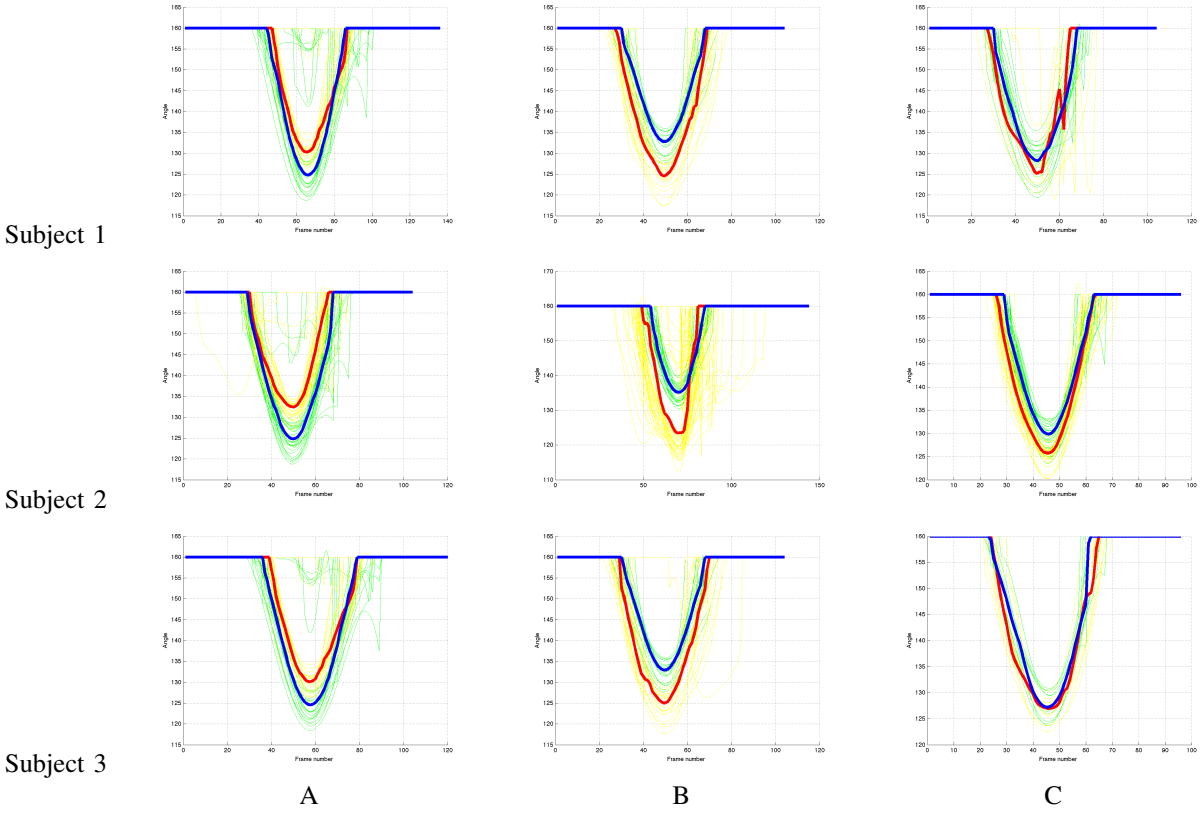

Fig. 3. Angle variations for 3 subjects. The red curve represents the mean cycle of right leg, while the blue one represents the mean cycle of left leg. (A) the person was wearing the heel cup under the left foot, producing a significant lower curve than the one of the right leg. (B) The situation was reversed, the heel cup was under the right foot, the red curve is lower than the right curve. (C) Without the heel cup, the two curves are alike.

structured light system, the Kinect camera. Requiring only one front-view image, our system detects very efficiently gait asymmetry thanks to a 3D skeleton model construction process. We have also shown that using only the information about the variation of the angle between the upper and lower legs was sufficient to detect and analyze abnormal gaits. More importantly, our gait analysis system is much less expensive than a MOCAP system and does not require wearable markers. In the future, we plan to assess the precision of our method by comparing it with a motion capture system.

REFERENCES

[1] J. Han and B. Bhanu, Individual recognition using gait energy image, IEEE Transactions on Pattern Analysis and Machine Intelligence, vol. 28, no. 2, 2006, pp. 316-322.

[2] R. Collins, A. Lipton, T. Kanade, H. Fujiyoshi, D. Duggins, Y. Tsin, D. Tolliver, N. Enomoto and O. Hasegawa, A System for Video Surveillance and Monitoring: VSAM Final Report, Technical report CMU-RI-TR-00- 12, Robotics Institute, Carnegie Mellon University, May 2000.

[3] A.L. McDonough, M. Batavia, F.C. Chen, S. Kwon and J. Zia, The validity and reliability of the GAITRite system's measurements: A preliminary evaluation, Arch Phys Med Rehabil, vol. 82, no. 3, 2001, pp. 419-425.

[4] B. Gurney, Leg length discrepancy. Gait & Posture, vol. 15, no. 2, 2002, pp. 195-206.

[5] T. Karaharju-Huisnan, S. Taylor, R. Begg, J. Cai and R. Best, Gait symmetry quantification during treadmill walking. The Seventh Australian and New Zealand 2001 Intelligent Information Systems Conference, 2001, pp. 203-206.

[6] H. Sadeghi, P. Allarda, F. Princea and H. Labelle, Symmetry and limb dominance in able-bodied gait: a review. Gait & Posture, vol. 12, no. 1, 2000, pp. 34-45.

[7] C. Rougier, E. Auvinet, J. Meunier, M. Mignotte, and J. de Guise, Depth energy image for gait symmetry quantification, EMBC, sept. 2011, pp. 5136-5139.

[8] F. Potdevin, C. Gillet, F. Barbier, Y. Coello and P. Moretto, The study of Asymmetry in Able-bodied Gait with the concept of Propulsion and Brake. 9th Symposium on 3D Analysis of Human Movement, Valenciennes, France, 2006.

[9] A. Sant Anna and N. Wickstrom, A Symbol-Based Approach to Gait Analysis From Acceleration Signals: Identification and Detection of Gait Events and a New Measure of Gait Symmetry, IEEE Transactions on Pattern Analysis and Machine Intelligence, vol. 14, no. 5, 2010, pp. 1180- 1187.

[10] J.P.Kuhtz-Buschbeck, K.Brockmann, R.Gilster, A.KochandH.Stolze, Asymmetry of arm-swing not related to handedness. Gait & Posture, vol. 27, no. 3, 2008, pp. 447-454.

[11] Microsoft kinect. Available: http://www.xbox.com/kinect

[12] Martin A. Fischler and Robert C. Bolles, Random Sample Consensus: A Paradigm for Model Fitting with Applications to Image Analysis and Automated Cartography, Comm. of the ACM, 24 (6): 381:395, 1981.

[13] Mathworld, http://mathworld.wolfram.com/LeastSquaresFittingPolynomial.html

[14] J. B. MacQueen (1967), Some Methods for classification and Analysis of Multivariate Observations, Proceedings of 5-th Berkeley Symposium on Mathematical Statistics and Probability, Berkeley. University of California Press, 1:281-297.

[15] E. C. R. Motmans, Anthropometry table ergonomie rc, DinBelg, Tech. Rep., 2005. [Online]. Available: www.dinbelg.be.

[16] E. Auvinet, F. Multon, and J. Meunier, Gait analysis with multiple depth cameras, EMBC, sept. 2011, pp. 6265-6268.